

Structural Changes of Diblock Copolymer Melts Due to an External Electric Field: A Self-Consistent-Field Theory Study

Chin-Yet Lin* and M. Schick

Department of Physics, University of Washington, Seattle, Washington 98195-1560

David Andelman

School of Physics and Astronomy, Raymond and Beverly Faculty of Exact Sciences, Tel Aviv University, Ramat Aviv 69978, Tel Aviv, Israel

Received February 25, 2005; Revised Manuscript Received April 29, 2005

ABSTRACT: We study the phase behavior of diblock copolymers in the presence of an external electric field. We employ self-consistent-field theory and treat the relevant Maxwell equation as an additional self-consistent equation. Because we do not treat the electric field perturbatively, we can examine its effects even when its magnitude is large. The electric field couples to the system's morphology only through the difference between the dielectric constants of the two blocks. We find that an external field aligns a body-centered-cubic phase along the (111) direction, reducing its symmetry group to $R\bar{3}m$. Transitions between this phase and the disordered or hexagonal phases can occur for external electric fields ranging from a minimum to a maximum value beyond which the $R\bar{3}m$ phase disappears completely. This electric field range depends on diblock architecture and temperature. We present several cuts through the phase diagram in the space of temperature, architecture, and applied field, including one applicable to a system recently studied.

I. Introduction

Because block copolymers readily self-assemble into various ordered arrays, they have been avidly studied for technological applications such as high-density porous materials, nanolithographic templates, photonic band gap materials,^{1–3} and well-ordered arrays of metal nanowires.^{1,4} One practical difficulty to their use in some applications is that the ordered phase is not created in one single crystal, but rather in domains of differing orientation. One means of aligning the domains is to apply an external electric field. It has been shown^{3,5–8} that applying an electric potential, on the order of a few to a few dozen volts across electrodes separated by several micrometers, can effectively orient domains of lamellar or cylindrical morphology normal to the surfaces of thin films. The basis of this orientation effect is simple. To reduce accumulation of polarization charge, the system lowers its free energy by aligning cylinders or lamellae so that their long axis is parallel to the applied field.

Recently, related experiments on diblock copolymers⁹ have been performed where external fields have been applied to bring about a phase transition from a phase of spheres to one of cylinders. In the phase of spheres, it is not possible to eliminate the accumulation of polarization charge so that its free energy increases in an external field with respect to a cylindrical phase, and a phase transition can be induced. This change in phase due to the application of an electric field was considered by Tsori et al.¹⁰ and by Xu et al.⁹

The effects of an external field on an ordered array of inhomogeneous dielectric material are of great interest. First, the problem is inherently self-consistent simply because the material is a dielectric; i.e. the electric field at a given point depends on the polarization

at that point which, in turn, depends on the local electric field. In addition, in the problem of interest here, the local dielectric constant is inhomogeneous. It depends on the morphology of the ordered phase, which itself depends upon the local electric field.¹¹

In previous calculations for diblock copolymers,^{9,10} this self-consistent circle has been broken by assuming that the two blocks are only weakly segregated, resulting in a small amplitude of the spatial variation of the relative concentration of the two blocks. In this case it follows from the vanishing of the divergence of the electric displacement that the amplitude of the spatially varying electric field is also small so that the electrostatic Maxwell equation can be solved perturbatively for the electric field as a function of the order parameter. This procedure was carried out to quadratic order in the field by Amundson et al.¹² It is appropriate in the weak-segregation limit and should be adequate for determining the general phase behavior in weak external fields. However, since experiments are often not in the weak segregation limit and the effect of electric fields has hardly been explored, further study is clearly called for.

In recent years, thermodynamic properties of block copolymer systems have been treated successfully by the *full* self-consistent-field (SCF) theory, to which weak- and strong-segregation theories are approximations.¹³ Given the self-consistent nature of an inhomogeneous dielectric in an external electric field, it seems natural to apply the full SCF theory to this problem as well. That is what we do in this paper. We solve exactly the full set of SCF equations and the appropriate Maxwell equations under the assumption of a simple constitutive relation between the local dielectric properties and the local volume fractions. In particular, we consider the evolution of the bulk phase diagram of diblock copolymers in an applied electric field and focus upon its effect on reducing the region of the phase diagram occupied by the body-centered-cubic (bcc) structure (space group

* Corresponding author. E-mail: chimney@u.washington.edu.

$Im\bar{3}m$). Evolution of the gyroid structure (space group $Ia\bar{3}d$), whose region in the phase diagram also decreases due to the application of a field, is not considered.

We calculate the strength of an external field needed to bring about a phase transition from the (distorted) spherical phase to the disordered phase and to the cylindrical phase. For the transition to the latter phase we find two distinct behaviors depending upon the architecture of the diblock, as measured by the parameter f_A introduced below. The first is brought about if a transition from the spherical phase to the cylindrical phase can be induced in the absence of an external electric field simply by reducing the temperature in the realm of interest. If so, the same must also be true for very small fields. As a consequence, one can always find a temperature in that realm at which an arbitrarily small field will induce a transition from the spherical to the cylindrical phase. The other behavior occurs if the spherical phase is the most stable one in the absence of an external field for temperatures in the realm of interest. In that case, a nonzero external field is required to induce a transition from it to the cylindrical one at any temperature in this realm. In either case, we find that for a given architecture there is a maximum value of applied field beyond which the spherical phase is no longer the most stable one for any temperature.

In the following section, we set up the general formalism. In section III, we discuss its application to the phase of (distorted) spheres and compare the results of the full self-consistent calculation with those obtained from an expansion of the free energy in the electric field to order E^2 . Such an expansion does not indicate the optimal direction in which the field aligns the cubic phase, whereas the full calculation shows that alignment along the (111) direction is favored over a (100) orientation. There is a concomitant reduction of the symmetry of the phase from $Im\bar{3}m$ (bcc phase) to $R\bar{3}m$ (distorted spherical phase). Various cuts through the phase diagram are also presented. We conclude with a brief summary and comparison with recent experiments.

II. General Formalism

We consider a melt of n A–B diblock copolymer chains, each of polymerization index $N = N_A + N_B$. If the specific volumes of the A and B monomers are v_A and v_B , respectively, the volume per chain is $v_p = N_A v_A + N_B v_B$. For an incompressible melt of A–B chains, the volume fraction of the A monomers is $N_A v_A / (N_A v_A + N_B v_B)$, and the total system volume is $\Omega = n v_p$. We assume the monomer volumes to be identical, $v_A = v_B$, so that the volume fraction of the A monomers is equal to the mole fraction of the A monomers, $f_A = N_A / N$. We also assume that the Kuhn lengths of the A and B components are identical, a length denoted a .

In the absence of an external field, the application of SCF theory¹⁴ leads to a free energy \mathcal{F} which is a functional of unknown fields W_A , W_B , and Ξ and a function of temperature T

$$\frac{\mathcal{F}(W_A, W_B, \Xi; T)}{n k_B T} \equiv -\ln \mathcal{Q}[W_A, W_B] + \frac{1}{\Omega} \int d\mathbf{r} \{ \chi N \Phi_A \Phi_B - W_A \Phi_A - W_B \Phi_B - \Xi (1 - \Phi_A - \Phi_B) \} \quad (1)$$

where k_B is the Boltzmann constant; $\Phi_A(\mathbf{r})$ and $\Phi_B(\mathbf{r})$ are the local volume fractions of A and B monomers. The dependence on T comes from the usual Flory interaction parameter, χ , which to a good approximation is inversely proportional to the temperature, $\chi N = b/T$ with b a constant. The function $\mathcal{Q}[W_A, W_B]$ is the partition function of a single polymer chain subject to the fields $W_A(\mathbf{r})$ and $W_B(\mathbf{r})$, as is given below. The field $\Xi(\mathbf{r})$ is a Lagrange multiplier that enforces locally the incompressibility constraint, $\Phi_A(\mathbf{r}) + \Phi_B(\mathbf{r}) = 1$. The three unknown fields are determined by requiring that the free energy functional be extremized with respect to their variation at constant T .

The fields W_A and W_B appear in the single-chain partition function of the flexible diblock copolymer, $\mathcal{Q}[W_A, W_B] = \int d\mathbf{r} q(\mathbf{r}, 1)/c$, where $q(\mathbf{r}, s)$ satisfies the modified diffusion equation

$$\frac{\partial q}{\partial s} = \frac{1}{6} N a^2 \nabla^2 q - W_A(\mathbf{r}) q, \quad \text{if } 0 \leq s \leq f_A \quad (2)$$

and

$$\frac{\partial q}{\partial s} = \frac{1}{6} N a^2 \nabla^2 q - W_B(\mathbf{r}) q, \quad \text{if } f_A < s \leq 1 \quad (3)$$

with the initial condition $q(\mathbf{r}, 0) = 1$, and c is a volume of no consequence here.

The addition of a local electric field $\mathbf{E}(\mathbf{r})$ in the derivation of the free energy \mathcal{F} is straightforward. In an ensemble for which an external electric potential is held fixed,¹⁵ the above free energy simply becomes

$$\frac{\mathcal{F}(W_A, W_B, \Xi; T, \mathbf{E})}{n k_B T} = -\ln \mathcal{Q}[W_A, W_B] - \frac{\epsilon_0 v_p}{k_B T} \int \frac{d\mathbf{r}}{2\Omega} \kappa(\mathbf{r}) |\mathbf{E}(\mathbf{r})|^2 + \frac{1}{\Omega} \int d\mathbf{r} \{ \chi N \Phi_A \Phi_B - W_A \Phi_A - W_B \Phi_B - \Xi (1 - \Phi_A - \Phi_B) \} \quad (4)$$

where ϵ_0 is the vacuum permittivity and $\kappa(\mathbf{r})$ is the local dielectric constant. A constitutive relation between $\kappa(\mathbf{r})$ and the volume fractions of A and B monomers must be specified. We choose the local dielectric constant to be given by its local average

$$\kappa(\mathbf{r}) = \kappa_A \Phi_A(\mathbf{r}) + \kappa_B \Phi_B(\mathbf{r}) \quad (5)$$

where κ_A and κ_B are the dielectric constants of pure A and B homopolymer phases, respectively. This choice is clearly correct in the limiting cases of the pure systems and in the weak-segregation limit. It also has the virtue of simplicity and should capture the essential physics.

From the above it can be seen that a convenient scale for the strength of the electric field is

$$\mathcal{E} \equiv \left(\frac{k_B T}{\epsilon_0 v_p} \right)^{1/2} \quad (6)$$

The magnitude of this electric field unit at typical experimental temperatures, $T \approx 430$ K, and for typical volume per polymer chain, $v_p \approx 100$ nm³, is $\mathcal{E} \approx 82$ V/ μ m. We shall denote the dimensionless electric field rescaled in this unit as $\hat{\mathbf{E}} \equiv \mathbf{E}/\mathcal{E}$. Similarly a dimensionless displacement field, $\hat{\mathbf{D}}$, is conveniently defined by $\hat{\mathbf{D}} \equiv \mathbf{D}/\epsilon_0 \mathcal{E}$.

The requirement that the free energy functional be an extremum with respect to variation of W_A , W_B , and Ξ and of the volume fractions Φ_A and Φ_B at constant temperature, or χN , and fixed electric field $\hat{\mathbf{E}}$ leads to the following set of SCF equations:

$$w_A = \chi N \phi_B + \xi - \frac{1}{2} \kappa_A |\hat{\mathbf{E}}|^2 \quad (7)$$

$$w_B = \chi N \phi_A + \xi - \frac{1}{2} \kappa_B |\hat{\mathbf{E}}|^2 \quad (8)$$

$$\phi_A + \phi_B = 1 \quad (9)$$

$$\phi_A = -\frac{\Omega}{\mathcal{Q}} \frac{\delta \mathcal{Q}}{\delta w_A} \quad (10)$$

$$\phi_B = -\frac{\Omega}{\mathcal{Q}} \frac{\delta \mathcal{Q}}{\delta w_B} \quad (11)$$

The values of W_A , W_B , Ξ , Φ_A , and Φ_B which satisfy these equations are denoted by lower case letters w_A , w_B , ξ , ϕ_A , and ϕ_B , respectively. The free energy within the SCF approximation, F_{scf} , is obtained by substitution of these values into the free energy of eq 4

$$F_{\text{scf}}(T, \mathbf{E}) = \mathcal{F}(w_A, w_B, \xi; T, \mathbf{E}) \quad (12)$$

or

$$\frac{F_{\text{scf}}}{nk_B T} = -\ln \mathcal{Q}[w_A, w_B] - \frac{1}{\Omega} \int d\mathbf{r} [\chi N \phi_A(\mathbf{r}) \phi_B(\mathbf{r}) + \xi(\mathbf{r})] \quad (13)$$

In addition to these equations, there are also the Maxwell equations which the electrostatic field must satisfy in absence of free charges:

$$\nabla \times \hat{\mathbf{E}} = 0 \quad (14)$$

$$\nabla \cdot \hat{\mathbf{D}}(\mathbf{r}) \equiv \nabla \cdot (\epsilon_0 \kappa(\mathbf{r}) \hat{\mathbf{E}}(\mathbf{r})) = 0 \quad (15)$$

As usual, we guarantee that the first of these equations is satisfied by introducing the electric potential $\hat{V}(\mathbf{r})$

$$\hat{\mathbf{E}}(\mathbf{r}) = -\nabla \hat{V}(\mathbf{r}) = -\nabla V(\mathbf{r}) / \mathcal{Q} \quad (16)$$

Since we will consider, in addition to the disordered phase, spatially periodic ones, it is convenient to write all functions of position in terms of their values averaged over a unit cell

$$C_0 \equiv \langle C \rangle = \frac{\int_{\text{unit cell}} C(\mathbf{r}) d\mathbf{r}}{\int_{\text{unit cell}} d\mathbf{r}} \quad (17)$$

and their deviations from those average values

$$\delta C(\mathbf{r}) \equiv C(\mathbf{r}) - C_0 \quad (18)$$

The average values of several quantities of interest are

$$\begin{aligned} \phi_{A,0} &= f_A \\ \phi_{B,0} &= 1 - f_A \\ \kappa_0 &= \kappa_A f_A + \kappa_B (1 - f_A) \end{aligned}$$

$$\begin{aligned} w_{A,0} &= \chi N (1 - f_A) - \frac{1}{2} \kappa_A |\hat{\mathbf{E}}_0|^2 \\ w_{B,0} &= \chi N f_A - \frac{1}{2} \kappa_B |\hat{\mathbf{E}}_0|^2 \end{aligned} \quad (19)$$

where the value of ξ_0 has been arbitrarily set to zero, and $\hat{\mathbf{E}}_0$ is the value of the local electric field averaged over a unit cell. To determine this without knowing the full spatially dependent electric field $\mathbf{E}(\mathbf{r})$, we reason as follows. Assume that the external field is produced by planar electrodes which are separated by a distance d and subject to a voltage difference V_{12} . In the gap, and along the z -axis perpendicular to the electrodes, the field is $E_{\text{ext}} = -V_{12}/L$. Given that the dielectric fills the space between the plates and that the voltage V_{12} is held fixed as the dielectric is inserted, it follows that $\int E_z dz = E_{\text{ext}} L$ and that the average value of E_z is E_{ext} . We make a reasonable assumption that the free energy of the system is minimized when an axis of symmetry of one of the ordered structures coincides with the z -axis. In this case $E_0 = \int_0^L E_z dz / L = E_{\text{ext}}$. Hence, in rescaled units

$$\hat{\mathbf{E}}_0 = \left(\frac{\epsilon_0 V_p}{k_B T} \right)^{1/2} E_{\text{ext}} \hat{\mathbf{z}} \quad (20)$$

and

$$\delta \hat{\mathbf{E}}(\mathbf{r}) = \hat{\mathbf{E}}(\mathbf{r}) - \hat{\mathbf{E}}_0 \equiv -\nabla \delta \hat{V}(\mathbf{r}) \quad (21)$$

Utilizing these average values, we can rewrite the free energy in the SCF approximation, eqs 12 and 13, in the form

$$\begin{aligned} \frac{F_{\text{scf}}}{nk_B T} &= -\ln \left\{ \frac{\mathcal{Q}[w_A, w_B]}{\mathcal{Q}[w_{A,0}, w_{B,0}]} \right\} + \chi N f_A (1 - f_A) - \\ &\quad \frac{1}{2} \kappa_0 \hat{E}_0^2 - \frac{\chi N}{\Omega} \int \delta \phi_A(\mathbf{r}) \delta \phi_B(\mathbf{r}) d\mathbf{r} \end{aligned} \quad (22)$$

where, from the incompressibility condition, $\delta \phi_A(\mathbf{r}) = -\delta \phi_B(\mathbf{r})$. Note that the electric field contribution $-\kappa_0 \hat{E}_0^2 / 2$ is common to all phases. For the lamellar and hexagonal phases in the lowest energy orientation, this is the *only* contribution to the free energy from the electric field. It can conveniently be absorbed in a redefinition of the free energy

$$f_n(\hat{E}_0) \equiv F_{\text{scf}} / nk_B T + \frac{1}{2} \kappa_0 \hat{E}_0^2 \quad (23)$$

The advantage of separating out the average values is that the only remaining Maxwell equation, eq 15, can be written as an *inhomogeneous* equation for the potential $\delta \hat{V}(\mathbf{r})$

$$\begin{aligned} \nabla \delta \hat{V}(\mathbf{r}) \cdot \nabla [\kappa_A \delta \phi_A(\mathbf{r}) + \kappa_B \delta \phi_B(\mathbf{r})] + [\kappa_A (f_A + \delta \phi_A(\mathbf{r})) + \\ \kappa_B (1 - f_A + \delta \phi_B(\mathbf{r}))] \nabla^2 \delta \hat{V}(\mathbf{r}) = \hat{E}_0 \frac{\partial}{\partial z} [\kappa_A \delta \phi_A(\mathbf{r}) + \\ \kappa_B \delta \phi_B(\mathbf{r})] \end{aligned} \quad (24)$$

This, and the three remaining self-consistent equations,

$$\begin{aligned} \delta w_A(\mathbf{r}) &= \chi N \delta \phi_B(\mathbf{r}) + \delta \xi(\mathbf{r}) + \\ &\quad \frac{1}{2} \kappa_A [2 \hat{\mathbf{E}}_0 \cdot \nabla \delta \hat{V}(\mathbf{r}) - (\nabla \delta \hat{V}(\mathbf{r}))^2] \end{aligned} \quad (25)$$

$$\begin{aligned} \delta w_B(\mathbf{r}) &= \chi N \delta \phi_A(\mathbf{r}) + \delta \xi(\mathbf{r}) + \\ &\quad \frac{1}{2} \kappa_B [2 \hat{\mathbf{E}}_0 \cdot \nabla \delta \hat{V}(\mathbf{r}) - (\nabla \delta \hat{V}(\mathbf{r}))^2] \quad (26) \\ \delta \phi_A(\mathbf{r}) + \delta \phi_B(\mathbf{r}) &= 0 \quad (27) \end{aligned}$$

constitute the four self-consistent equations which determine the four functions $\delta w_A(\mathbf{r})$, $\delta w_B(\mathbf{r})$, $\delta \xi(\mathbf{r})$, and $\delta \hat{V}(\mathbf{r})$.

We note that with our choice of constant external field applied along the z direction the Maxwell equation, eq 24, admits the following symmetry:

$$\begin{aligned} \delta \hat{V}(\mathbf{r}_{\perp}, z) &= \delta \hat{V}(-\mathbf{r}_{\perp}, z) = -\delta \hat{V}(\mathbf{r}_{\perp}, -z) \\ \kappa(\mathbf{r}_{\perp}, z) &= \kappa_A \phi_A(\mathbf{r}_{\perp}, z) + \kappa_B \phi_B(\mathbf{r}_{\perp}, z) \\ &= \kappa(-\mathbf{r}_{\perp}, z) = \kappa(\mathbf{r}_{\perp}, -z) \quad (28) \end{aligned}$$

where the components of \mathbf{r} have been written as (\mathbf{r}_{\perp}, z) . The self-consistent equations, eqs 24–27, are now solved by a standard procedure of expanding the functions of position in a complete set of functions with the above symmetries and those of any specific phase considered.¹³ We have utilized in our calculation sets of basis functions containing between 70 and 125 functions, depending upon the value of χN .

The only parameters entering our calculation are χN , f_A , κ_A , and κ_B and the rescaled external field $E_{\text{ext}}/\mathcal{E}$. Comparison of the results with experiment requires the evaluation of \mathcal{E} for given T and volume per chain v_p . In addition, the relation between T and χN must be specified.

III. Results

As noted earlier, the free energies of lamellar or hexagonal phases are minimized when the lamellae or the cylinders are aligned parallel to the electric field because in this orientation there is no buildup of polarization charge. In the body-centered-cubic (bcc) phase, however, there must be an accumulation of polarization charge irrespective of the external field direction. We must determine which field direction produces a phase of distorted spheres with the lowest free energy and how large a field this phase can sustain before a transition to the hexagonal phase is encountered. It is these issues which we now address.

A. The $R\bar{3}m$ to Hexagonal Phase Transition. The symmetry group of the bcc phase is $Im\bar{3}m$, which has three two-dimensional space subgroups: $p4mm$ along the [100] direction, $p6mm$ along the [111] direction, and $p2mm$ along the [110] direction. If the field were applied along either the [110] or [100] directions, the symmetry would be reduced to $I4/mmm$, while if it were applied along the [111] direction, the symmetry would be reduced to $R\bar{3}m$. The symmetry in the latter case is of a bcc arrangement of spheres that has been distorted along the [111] direction. As the $R\bar{3}m$ group has the $p6mm$ symmetry of the hexagonal phase, one would suspect that a field applied along the diagonal [111] direction will result in the lowest free energy. By direct calculation of these configurations, we find that the $R\bar{3}m$ phase does indeed have a lower free energy than that of the $I4/mmm$.

That the electric field favors one orientation of the $Im\bar{3}m$ over another is an effect which is not captured

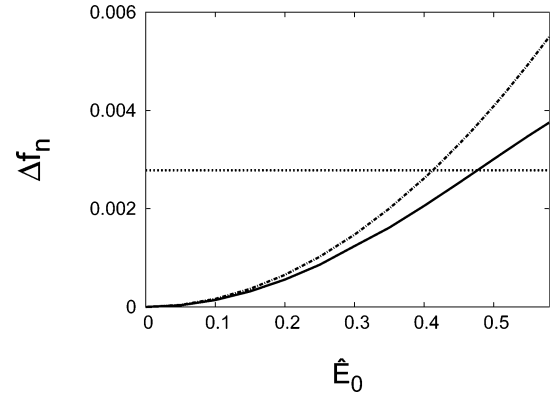


Figure 1. The difference, Δf_n , between the dimensionless free energy, f_n , defined in eq 23 and its value in zero external field in the bcc phase. It is calculated from the SCF theory and is plotted vs dimensionless external electric field, $\hat{E}_0 = E_0/\mathcal{E}$, for the hexagonal phase (horizontal dotted line) and the $R\bar{3}m$ phase (solid line). The system is characterized by a $\chi N = 15$, $f_A = 0.29$. The dielectric constants are $\kappa_A = 6.0$ (for the PMMA block) and $\kappa_B = 2.5$ (for the PS block), yielding $\kappa_0 \approx 3.52$. The perturbation theory result for the $R\bar{3}m$ phase is shown as a dashed and dotted line. It has a higher free energy.

by an expansion of the free energy to quadratic order in the external field.¹¹ Nonetheless, it is instructive to consider the result of such an expansion. It is obtained by solving the Maxwell equation $\nabla \cdot [\epsilon_0 \kappa(\phi_A, \phi_B) \mathbf{E}] = 0$ to second order in \mathbf{E} to obtain $\mathbf{E}(\phi_A, \phi_B)$ and evaluating this field from the volume fractions characterizing the system in the absence of an external field. The distortion of the density distribution produced by this field itself contributes terms to the free energy which are higher order in E^2 . For a phase which is cubic in the absence of an electric field, the perturbation result can be written as¹²

$$\begin{aligned} \frac{F_{\text{pt}}(\hat{E}_0)}{nk_B T} &= -\frac{1}{2} \kappa_0 \hat{E}_0^2 \left[1 - \frac{1}{12\Omega} \left(\frac{\kappa_A - \kappa_B}{\kappa_0} \right)^2 \int d\mathbf{r} [\delta \phi_A(\mathbf{r}) - \delta \phi_B(\mathbf{r})]^2 \right] \\ &\equiv -\frac{1}{2} \kappa_{\text{eff}} \hat{E}_0^2 \quad (29) \end{aligned}$$

where $\delta \phi_A = -\delta \phi_B$ is the variation of the local volume fraction in the zero-field structure and κ_{eff} is, by definition, the effective dielectric constant for the structure in the field.

We now compare the full SCF solution with this perturbation result. We choose $\chi N = 15$ and $f_A = 0.29$, values at which the bcc phase is the most stable in zero electric field. The dielectric constants are chosen to make contact with recent experimental systems of poly(methyl methacrylate) (PMMA)/polystyrene (PS) diblock copolymer, which is referred to hereafter as the PMMA–PS system. At experimental temperatures around 160 °C the dielectric constants appropriate to the PMMA–PS copolymer with PMMA being the A block and PS the B block are $\kappa_A = 6.0$ (for PMMA) and $\kappa_B = 2.5$ (for PS),^{5,9,10} which yield an average of $\kappa_0 \approx 3.52$. In Figure 1, we show the difference, Δf_n , between the free energy $f_n(\hat{E}_0) \equiv F_{\text{scf}}/nk_B T + \kappa_0 \hat{E}_0^2/2$, eq 23, and its value in zero external field in the bcc phase. It is shown as a function of \hat{E}_0 , for the hexagonal phase and for the $R\bar{3}m$ phase, as calculated from the full SCF theory and from

perturbation theory. The latter is seen to be adequate for fields smaller than 10–20% of the natural unit \mathcal{E} at which $\hat{E}_0 = 1$. The figure also shows that there is a transition from the $R\bar{3}m$ to the hexagonal phase at a value of $\hat{E}_0 \approx 0.477$ as determined from the full self-consistent calculation. Perturbation theory underestimates the magnitude of the field needed to bring about this transition. That the transition is first-order is easily seen as follows. The average electric and displacement fields, E_0 and D_0 , are evaluated by taking their spatial averages over the unit cell. In our case the only nonzero average components are those in the z -direction, and they are related to the free energy per unit volume according to

$$\frac{\partial F/\Omega}{\partial E_0} = -D_0 \quad (30)$$

or

$$\frac{\partial F/nk_B T}{\partial \hat{E}_0} = -\hat{D}_0 \quad (31)$$

One sees from Figure 1 that at the phase transition the free energies of the $R\bar{3}m$ and hexagonal phases intersect with different slopes; therefore, the displacement field changes abruptly.

As a result of the application of the electric field along the [111] direction, the spheres of minority component are elongated in this direction. A density profile of the system in the $R\bar{3}m$ phase at an external field $\hat{E}_0 = 0.470$, slightly smaller than that at the transition to the hexagonal phase, $\hat{E}_0 = 0.477$, is shown in Figure 2b. At the transition, the profile changes abruptly to that of the hexagonal phase, which is also shown in Figure 2c for $\hat{E}_0 = 0.480$. To see the extent of the distortion in the $R\bar{3}m$ phase, which can be characterized by the aspect ratio of the distorted spheres, 1.248, we also present the density profile of the bcc phase in zero external field, in Figure 2a. The cuts are in the plane containing the [111] and $[\bar{1}10]$ directions.

There are two features of interest that can be seen particularly clearly from the approximate expression of eq 29. The first is that in the $R\bar{3}m$ phase the effective average dielectric constant, κ_{eff} , is smaller than κ_0 . In the hexagonal and disordered phases, however, κ_{eff} is precisely κ_0 . Therefore, the displacement field D_0 in the $R\bar{3}m$ phase is smaller than in the other two phases. This is in accord with the change of slope of the free energy with electric field shown in Figure 1 and eqs 30 and 31.

The second concerns the fact that the dielectric constants are temperature-dependent. Therefore, the value of the electric field needed to bring about a phase transition will also vary with temperature. The perturbation expression leads one to expect that, for fields smaller than or comparable to \mathcal{E} , the natural E -field scale, the field at the transition will vary as

$$E_{\text{tr}}(T) \propto \frac{[\kappa_0(T)]^{1/2}}{\kappa_A(T) - \kappa_B(T)} = \frac{[f_A \kappa_A(T) + (1 - f_A) \kappa_B(T)]^{1/2}}{\kappa_A(T) - \kappa_B(T)} \quad (32)$$

B. The Generalized Clausius–Clapeyron Equation. Before presenting the phase diagram of our A/B block copolymer system in an E -field, we will make use of some general thermodynamic considerations. In

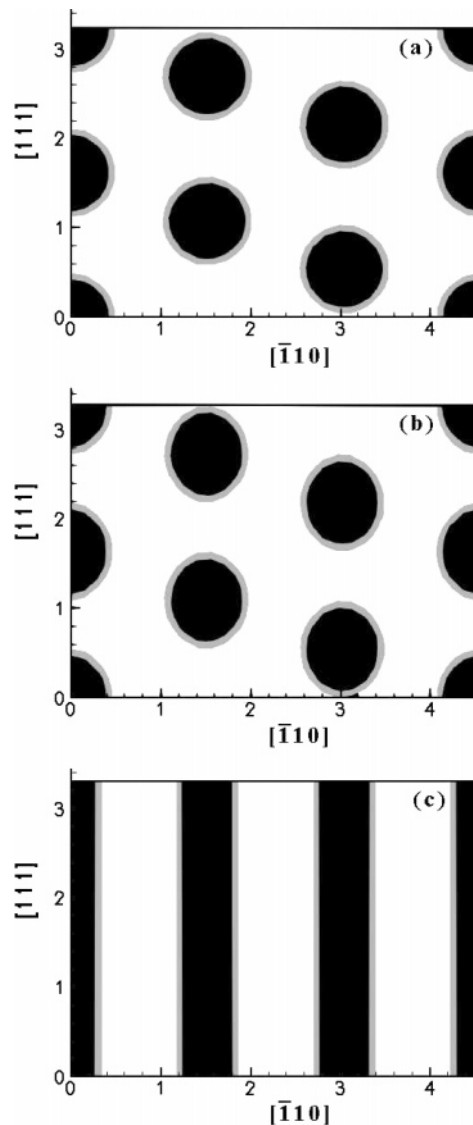


Figure 2. Density profiles for three different phases of a system characterized by $\chi N = 15$ and $f = 0.29$, with other parameters as in Figure 1: (a) the bcc phase which occurs in zero external field; (b) the $R\bar{3}m$ phase at an external electric field $\hat{E}_0 = 0.470$ just below the phase transition to the hexagonal phase which occurs at $\hat{E}_0 = 0.477$; (c) the hexagonal phase, which is shown for $\hat{E}_0 = 0.480$. The cuts are in the plane containing the [111] and $[\bar{1}10]$ directions. In the black regions, the local volume fractions of component A is greater than 0.55, in the intermediate regions, it is between 0.55 and 0.45, and in the white regions, it is less than 0.45.

particular, from the differential of the free energy per unit volume

$$d(F/\Omega) = -s dT - D_0 dE_0 \quad (33)$$

where $s = S/\Omega$ is the entropy per unit volume, one immediately derives a Clausius–Clapeyron equation for the slope of the coexistence line between any two phases

$$\frac{dE_0}{dT} = -\frac{\Delta s}{\Delta D_0} \quad (34)$$

where Δs and ΔD_0 are the differences in entropies and displacement fields, respectively, in the coexisting phases.

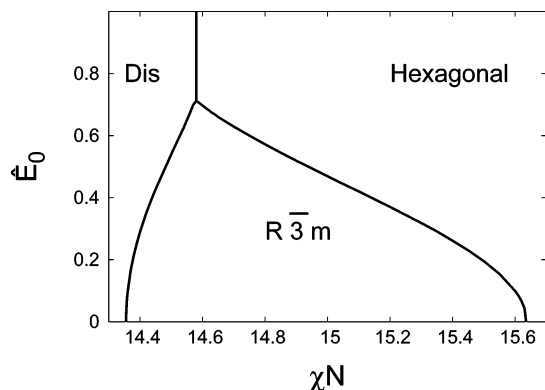


Figure 3. Calculated phase diagram of a diblock copolymer with a volume fraction of $f_A = 0.29$ in the presence of an external electric field. The phase diagram is shown as a function of the dimensionless field \hat{E}_0 and the interaction parameter χN . The triple point is located at $\hat{E}_{0,\text{triple}} = 0.71$ and $\chi N_{\text{triple}} = 14.58$. Other parameters as in Figure 1.

This can be expressed in terms of \hat{E}_0 , \hat{D}_0 , and $\chi N = b/T$ as

$$\frac{d\hat{E}_0}{d(\chi N)} = \frac{v_p}{\chi N} \frac{\Delta(s/k_B)}{\Delta\hat{D}_0} + \frac{\hat{E}_0}{2\chi N} \quad (35)$$

C. Phase Diagrams. We now turn to the phase diagram as a function of the inverse temperature, χN , the A-monomer fraction, f_A , and the applied external field, $\hat{E}_0 = E_0/\mathcal{E}$. We concentrate on the portion of the phase diagram involving the phase with $R\bar{3}m$ symmetry and the neighboring disordered and hexagonal phases. In the space of inverse temperature χN , the fraction f_A , and applied field, the $R\bar{3}m$ phase occupies a volume which is bounded by two sheets of first-order transitions: one from the $R\bar{3}m$ to the hexagonal phase and the other from the $R\bar{3}m$ to the disordered phase. These two sheets of first-order transitions meet at a line of triple points, $[\hat{E}_{0,\text{triple}}(f_A), \chi N_{\text{triple}}(f_A)]$. Beyond this line, the $R\bar{3}m$ phase no longer exists, while the disordered and hexagonal phases remain. They are separated by another sheet of first-order transitions which emerges from the line of triple points. Hence, this line is the locus at which all three sheets of first-order transitions meet.

In Figure 3 we show a cut through the phase diagram at fixed A-monomer fraction, $f_A = 0.29$. The cut shows the phase diagram as a function of the dimensionless electric field \hat{E}_0 and χN . At zero external field, the entropy difference between the bcc phase and the hexagonal phase is nonzero, but the difference in displacement field obviously vanishes. From the Clausius–Clapeyron equation, eq 35, the slope of the phase boundary between these two phases must be infinite at zero E -field. The same is true for the slope of the phase boundary between the bcc phase and the disordered phase at vanishing E -fields. Furthermore, we know from the zero electric field results that the entropy of the disordered phase is greater than that of the bcc phase which, in turn, is greater than that of the hexagonal phase. We also know that the displacement field in the disordered and in the hexagonal phases is equal to $\kappa_0 \epsilon_0 E_0$. As we noted earlier, the displacement field in the $R\bar{3}m$ phase is less than this value. This information, together with the Clausius–Clapeyron, eq 35, implies that the phase boundary between $R\bar{3}m$ and the disordered phase has a positive slope, while that between $R\bar{3}m$ and the hexagonal phase is negative in accord with Figure 3.

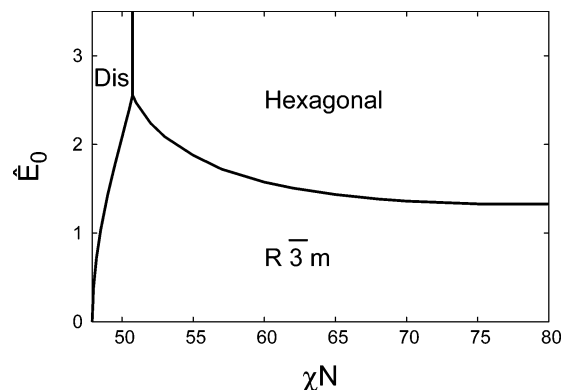


Figure 4. Calculated phase diagram of a diblock copolymer in the presence of an external electric field. Similar to Figure 3 but with fraction of the A block, $f_A = 0.1$. The phase diagram is shown as a function of the dimensionless field \hat{E}_0 and the interaction parameter χN . The triple point is located at $\hat{E}_{0,\text{triple}} = 2.56$ and $\chi N_{\text{triple}} = 50.74$.

Moreover, because of the presence of the positive second term in eq 35, the positive slope of the phase boundary between disordered and $R\bar{3}m$ phases will be greater in magnitude, or steeper, than that between the $R\bar{3}m$ and hexagonal phases. This is borne out by Figure 3. The three phases meet at the triple point, above which the phase boundary is vertical as there is no difference between the displacement fields of the coexisting disordered and hexagonal phases. The value of the electric field at the triple point is $\hat{E}_{0,\text{triple}} \approx 0.71$.

To make contact with experiment, we take parameters to fit the PMMA–PS system of ref 4. With $f_A = 0.29$ and a molecular mass of 3.9×10^4 g/mol, and utilizing the known values of monomeric volumes, we obtain a chain length of $N \approx 379$ and a volume per PMMA–PS chain of $v_p = 61.24$ nm³. At $T = 430$ K this yields $\mathcal{E} \equiv (k_B T / \epsilon_0 v_p)^{1/2} = 104.6$ V/ μm . Therefore, the value of the electric field at the triple point is in physical units $E_{0,\text{triple}} \approx 74.5$ V/ μm at this value of f_A and T . One sees from the figure that a transition from $R\bar{3}m$ to hexagonal phases could be brought about at electric fields within the interval from this maximum value down to zero, depending upon the values of χN and f_A .

The evolution of the phase diagram of Figure 3 with A-monomer fraction, f_A , is easily understood. As f_A decreases from 0.29, the phase boundary at zero field between $R\bar{3}m$ and hexagonal phases moves toward greater values of χN as does the boundary between disordered and $R\bar{3}m$ phases. When f_A is smaller than $f_A^{\text{coex}} = 0.114$, the value at which the bcc and hexagonal phases coexist at infinite χN ,¹⁶ the boundary between hexagonal and $R\bar{3}m$ phases will asymptote with zero slope to an f_A -dependent finite value as χN increases without limit. This zero slope also follows from the Clausius–Clapeyron eq 35 due to the fact that the ratio $\Delta s / \Delta \hat{D}_0$ is finite and $1/\chi N \rightarrow 0$.

An example of such a phase diagram is shown in Figure 4. This figure corresponds to a system with $f_A = 0.1 < f_A^{\text{coex}} = 0.114$, as was investigated recently in ref 9. In contrast with Figure 3, one sees here that the interval over which a transition can be observed from $R\bar{3}m$ to hexagonal phases now extends from the triple point at $\hat{E}_0 = 2.56$ down to a nonzero minimum value of $\hat{E}_0 = 1.33$. That is, for electric fields less than this minimum value, no transition from the $R\bar{3}m$ to a hexagonal phase occurs within our model. For PMMA–PS with $f_A = 0.1$ and molecular mass of 1.51×10^5 g/mol,

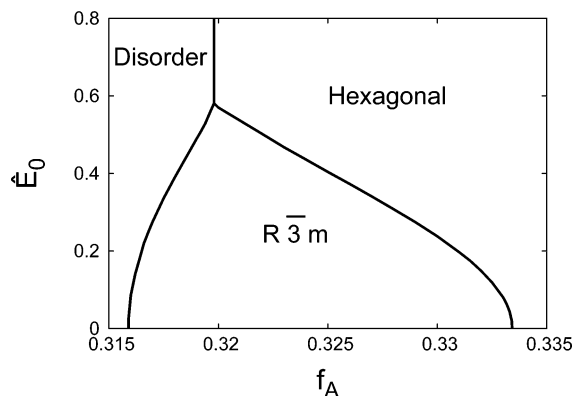


Figure 5. Calculated phase diagram for a diblock copolymer as a function of dimensionless external field and the A mole fraction parameter, f_A . Other parameters are $\chi N = 13.3$, $\kappa_A = 6.0$, and $\kappa_B = 2.5$. The triple point occurs at $\hat{E}_{0,\text{triple}} = 0.58$ and $f_{A,\text{triple}} = 0.32$.

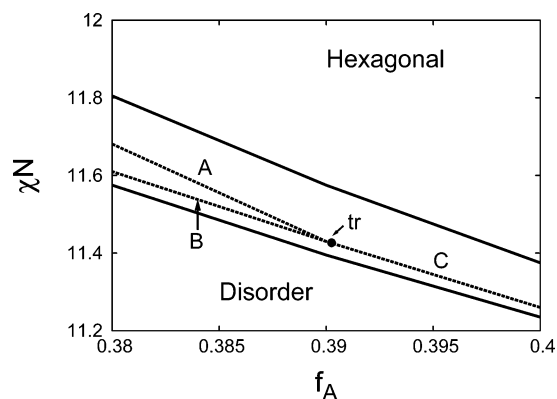


Figure 6. Calculated phase diagram at constant electric field, \hat{E}_0 . The outer two solid lines are the $E_0 = 0$ disorder-to-bcc and bcc-to-hexagonal phase boundaries. Between them we show three other transition lines for $\hat{E}_0 = 0.2$. They are the $R\bar{3}m$ -to-hexagonal (A), $R\bar{3}m$ -to-disorder (B), and disorder-to-hexagonal transition (C). These three lines meet at tr , the triple point: $f_{A,\text{triple}} = 0.390$ and $\chi N_{\text{triple}} = 11.43$.

as in ref 9, we obtain $N \approx 1458$ and a volume per chain $v_p = 239.7 \text{ nm}^3$. Therefore, at the experimental temperature of $T = 430 \text{ K}$, the unit of electric field $\mathcal{E} = 52.9 \text{ V}/\mu\text{m}$. In physical units, then, the triple point occurs at an external field of about $135 \text{ V}/\mu\text{m}$, and the minimum electric field needed to produce a transition can be estimated to be $79 \text{ V}/\mu\text{m}$.

In Figure 5 we show a different cut through the phase diagram in the (\hat{E}_0, f_A) plane and for a fixed $\chi N = 13.3$. The location of the triple point is $\hat{E}_{0,\text{triple}} = 0.58$ and $f_{A,\text{triple}} = 0.320$. This figure, and that of Figures 3 and 4, show that the value of the electric field needed to bring about a transition from the $R\bar{3}m$ phase is, for a given f_A fraction, a sensitive function of temperature and, for a given temperature, a sensitive function of the mole fraction of A block, f_A .

Figure 6 shows two cuts through the phase diagram at constant electric field, $\hat{E}_0 = 0$, and $\hat{E}_0 = 0.2$. The solid line at lower χN shows the phase boundary at zero-field between disordered and bcc phases while the solid line at larger χN shows the zero-field phase boundary between the bcc and hexagonal phases. The dashed lines between them show the phase boundaries for $\hat{E}_0 = 0.2$. The line denoted B is the boundary between the disordered and the $R\bar{3}m$ phase of distorted spheres; A is the boundary between $R\bar{3}m$ and hexagonal phases. These boundaries meet at the triple point, tr , which

occurs at $\chi N_{\text{triple}} \approx 11.43$ and $f_{A,\text{triple}} \approx 0.39$. For larger values of f_A , there is a line, C, of transitions directly from the disordered to the hexagonal phase. As the external field increases still further, the triple point recedes to larger values of χN , leaving behind only the line of direct transitions between disordered and hexagonal phases. Note that, except for the location of its terminus at the triple point, this boundary is independent of the applied field as it contributes to the free energy of both of these phases equally. The dielectric constants used to generate this figure are the same as those used in previous figures.

For completeness, we have also examined the case in which the dielectric constants of the minority and majority components are interchanged as compared with Figure 3. Namely, the majority component with $f_A = 0.71$ has the larger dielectric constant of $\kappa_A = 6.0$ and the minority the smaller value of $\kappa_B = 2.5$. We find that the $R\bar{3}m$ phase is now somewhat more stable with respect to the hexagonal phase, so that the value of the external electric field needed to bring about a transition from the former to the latter phase is increased. We note that this interchange increases the average value of the dielectric constant, so that all phases have a lower free energy due to the factor of $-\kappa_0 \hat{E}_0^2/2$ which it contains. However, it is not a priori obvious that the $R\bar{3}m$ phase would have its free energy lowered by more than that of the hexagonal phase by this interchange. In addition, we have determined that the spheres of minority component and lower dielectric constant distort in the [111] direction just as in the case when the minority component has the larger dielectric constant. The above effects are not captured by the perturbation result of eq 29 which is invariant under the interchange of κ_A and κ_B .

IV. Concluding Remarks

In sum, we have calculated the phase diagram of a block copolymer system in an external electric field which couples to the diblocks through the difference in their dielectric constants. We have employed a fully self-consistent-field approach in which the relevant Maxwell equation is treated on an equal footing with the other self-consistent equations. We have determined that the body-centered-cubic phase will preferentially align along the [111] direction, causing its symmetry to be reduced to $R\bar{3}m$. The electric field can induce phase transitions between this phase and either the disordered or the hexagonal phase. The strength of the field needed to induce such transitions is a sensitive function of the parameters of the system, such as its temperature and its chain architecture, which in the case of linear diblocks is quantified simply by the mole fraction, f_A .

For parameters that fit the experimental PMMA-PS diblock copolymer system investigated recently,⁹ $f_A = 0.1$, $v_p = 239.7 \text{ nm}^3$, and $T = 430 \text{ K}$, we find that an electric field of at least $70\text{--}80 \text{ V}/\mu\text{m}$ would be needed to observe a transition to the hexagonal phase. This contrasts with the reported existence of such a phase transition under an applied field of only $40 \text{ V}/\mu\text{m}$. There are several possible explanations of the difference between the experimental results and the theoretical ones presented here.

Our model employs a linear constitutive relation between dielectric constant and volume fractions and characterizes the PMMA-PS system by a few general parameters, the PMMA mole fraction f_A and the inter-

action parameter χN . It further assumes equal volumes for both monomers and equal Kuhn lengths for them. One knows that deviations from the last assumption certainly shift the locations of the phase boundaries.¹⁷ It is plausible that at rather asymmetric volume fractions of $f_A = 0.1$ the model provides only semiquantitative agreement with the experimental PMMA–PS phase diagram. Any difference in the theoretical and experimental phase diagrams at zero electric field will, in the presence of a nonzero one, manifest itself in a difference in relative stability of the various phases. Given the sensitive dependence on the phase boundaries of the minimum external field needed to bring about a phase transition, differences between the general theory and the experimental result are to be expected. At present, the phase diagram of the PMMA–PS system of ref 9 is not yet known. When additional experimental information becomes available, one will also need to determine the relationship between the temperature and the χN interaction parameter in order to convert the phase diagram calculated here to practical units so that it can be compared directly to the experimental one.

Last, we have employed a simple coupling between the system and the external field via the difference in dielectric constants of the copolymer blocks. Other couplings are possible.^{18,19} Just such an additional coupling, to mobile ions, has been suggested by Tsori et al.¹⁰ and is discussed also in ref 9. A minute fraction of mobile ions embedded in the minority PMMA fraction and not in the majority PS can lead to an enhanced response of the PMMA–PS system to external electric fields with moderate magnitude. It could also change the phase diagram quantitatively, resulting in a substantial lowering of the triple-point value of the electric field. Additional experiments, particularly on copolymers with the same PMMA–PS blocks, but at different temperatures or values of the architectural parameter f_A , would be most useful to shed additional light on the comparison of theory and experiment. In particular, a comparison of the two PMMA–PS systems of refs 4 and 9 would be enlightening because, as Figures 3 and 4 show, they are predicted here to exhibit significantly different phase behavior in an external electric field.

Acknowledgment. We are indebted to Ludwik Leibler, Tom Russell, Yoav Tsori, and Ting Xu for illuminating exchanges. Partial support from the National Science Foundation under Grant No. 0140500, the National Science Foundation IGERT fellowship from the University of Washington Center of Nanotechnology, the United States–Israel Binational Science Foundation (BSF) under Grant No. 287/02, and the Israel Science Foundation under Grant No. 210/01 is gratefully acknowledged.

References and Notes

- (1) Park, M.; Harrison, C.; Chaikin, P. M.; Register, R. A.; Adamson, D. H. *Science* **1997**, *276*, 1401.
- (2) Walheim, S.; Schaffer, E.; Mlynek, J.; Steiner, U. *Science* **1999**, *283*, 520.
- (3) Morkved, T.; Lu, M.; Urbas, A. M.; Ehrichs, E. E.; Jaeger, H. M.; Mansky, P.; Russell, T. P. *Science* **1996**, *273*, 931.
- (4) Thurn-Albrecht, T.; Schotter, J.; Kastle, G. A.; Emley, N.; Shibauchi, T.; Krusin-Elbaum, L.; Guarini, K.; Black, C. T.; Tuominen, M. T.; Russell, T. P. *Science* **2000**, *290*, 2126.
- (5) Thurn-Albrecht, T.; DeRouchey, J.; Russell, T. P. *Macromolecules* **2000**, *33*, 3250.
- (6) Böker, A.; Knoll, A.; Elbs, H.; Abetz, V.; Müller, A. H. E.; Krausch, G. *Macromolecules* **2002**, *35*, 1319.
- (7) Böker, A.; Elbs, H.; Hänsel, H.; Knoll, A.; Ludwigs, S.; Zettl, H.; Zvelindovsky, A.; Sevink, G. J. A.; Urban, V.; Müller, A. H. E.; Krausch, G. *Macromolecules* **2002**, *35*, 1319.
- (8) Tsori, Y.; Andelman, D. *Macromolecules* **2002**, *35*, 5161.
- (9) Xu, T.; Zvelindovsky, A.; Sevink, G.; Gang, O.; Ocko, B.; Zhu, Y.; Gido, S.; Russell, T. P. *Macromolecules* **2004**, *37*, 6980.
- (10) Tsori, Y.; Tournilhac, F.; Andelman, D.; Leibler, L. *Phys. Rev. Lett.* **2003**, *90*, 145504.
- (11) Amundson, K.; Helfand, E.; Quan, X.; Hudson, S. D.; Smith, S. D. *Macromolecules* **1994**, *27*, 6659.
- (12) Amundson, K.; Helfand, E.; Quan, X.; Smith, S. D. *Macromolecules* **1993**, *26*, 2698.
- (13) Matsen, M. W.; Schick, M. *Phys. Rev. Lett.* **1994**, *72*, 2660.
- (14) Schmid, F. *J. Phys.: Condens. Matter* **1998**, *10*, 8105.
- (15) Landau, L.; Lifshitz, E.; Pitaevskii, L. *Electrodynamics of Continuous Media*; Pergamon Press: Oxford, 1984.
- (16) Matsen, M. W.; Whitmore, M. *J. Chem. Phys.* **1996**, *105*, 9698.
- (17) Matsen, M. W.; Schick, M. *Macromolecules* **1994**, *27*, 4014.
- (18) Gurovich, E. *Macromolecules* **1994**, *27*, 7063.
- (19) Onuki, A.; Fukuda, J. *Macromolecules* **1995**, *28*, 8788.

MA050408M